MATEMATIKA, 2010, Volume 26, Number 1, 15–31

Mathematical Modeling of Tidal Circulation and Sediment Transport in the Gulf of Kachchh, West Coast of India

[1]P.C. Sinha, [2]G.K. Jena, [2]Indu Jain, [2]A.D. Rao & [1]Loy Kak Choon

[1]Institute of Oceanography, University of Malaysia Terengganu,
21030 Kuala Terengganu, Malaysia

[2]Centre for Atmospheric Sciences, Indian Institute of Technology Delhi
Hauz Khas, New Delhi – 110 016, India

e-mail: pcsinha@umt.edu.my

Abstract A multilevel breadth-averaged numerical model has been developed to study the tidal circulation, salinity and suspended sediment transport in the gulf of Khambhat along the west coast of India. The model is fully non-linear and uses a semi-explicit finite difference scheme to solve mass, momentum and advection diffusion equations in a vertical plane. A turbulent kinetic energy scheme is used to parameterize the vertical transfer of momentum, salinity and suspended sediments. The model is forced by prescribing the tidal elevations along the seaward open boundary of the analysis region. The tide in the gulf is mainly represented in the model by the semi-diurnal M_2 constituent. Numerical experiments are carried out to compute the tidal circulation, salinity intrusion and suspended sediment transport in the gulf region.

Keywords Numerical model; turbulent kinetic energy; tidal circulation; salinity; suspended sediment and gulf of Kachchh.

1 Introduction

The gulf of Kachchh is a semi-enclosed water body, located between the Rann of Kachchh, an embayment, and the Saurashtra peninsula, cental west coast of India. The gulf is the northeastern arm of the Arabian Sea, reaching eastward for approximately 170 km. Its width varies between approximately 20 and 80 kms. Its 350 km long coastline is rimmed with mudflats. The maximum depth of the gulf is 60m and numerous small islands are found in its water (Figure 1). The gulf has an average tidal range of 4 m which increases from the mouth to the head. Near the mouth, at Okha, the mean spring tidal range is 3.06 m and near the head, at Kandla, it is 5.88 m. The Central Electricity Authority [1] reported that the peak surface current velocity is in the range of 0.75-1.25 ms^{-1} at the mouth and 1.5-2.5 ms^{-1} in the central portion of the gulf.

Several researchers have developed numerical models for the study of circulation, salinity intrusion and sediment transport in the coastal and estuarine waters. Johns and Oguz [2] developed a numerical model for the exchange of water between the Black Sea and Marmara Sea through the Bosphorus. The multi-level two-dimensional model uses a turbulence parameterization which is based on Johns [3]. A transport equation has been added to study the salinity structure in the channel. The model results have basically shown a two-layer flow in the strait. Johns et al. [4] used a numerical model to determine changes in bed morphology resulting from the bed load and suspended transport of sand in the Taw estuary, England. Recently, Liu et al. [5] developed a laterally integrated two-dimensional hydrodynamic and salt water intrusion numerical model. The model was applied to the Tanshui river estuary to simulate the salinity distributions under different bathymetric configurations and for several scenarios of river flows. Prandle [6] studied the tidal currents

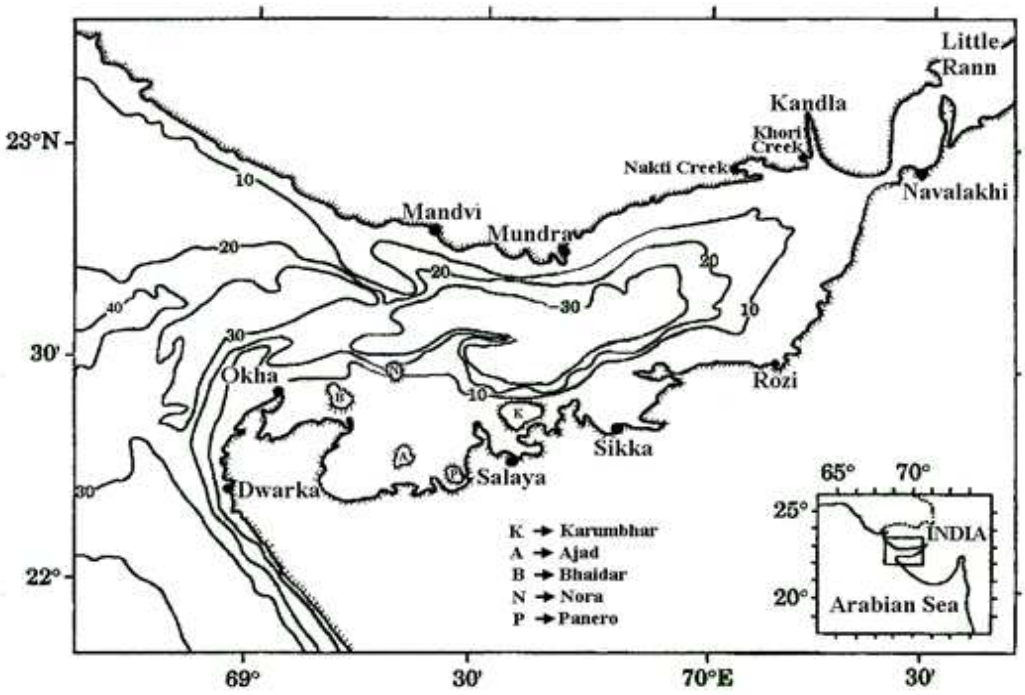

Figure 1: Map of the Gulf of Kachchh

and temporal and vertical variation of salinity intrusion by using a single-point numerical model in partially mixed estuaries. Chen [7] applied a laterally averaged model to compute hydrodynamics and salt transport in the Alafia river, Florida.

The principal objective of this study is to develop a breadth-averaged numerical model to study the circulation, salinity intrusion and suspended sediment transport in the gulf of Khambhat, west coast of India. The tidal current is computed in a vertical transect at three levels (surface, mid-depth and bottom) and at three locations (seaward, mid-way and landward) of the analysis area. The seaward, mid-way and landward stations correspond to approximately 68.93^0 E, 69.48^0 E and 70.04^0 E. The computed salinity results have been validated with the available observed values at some specific locations. During both the flood and the ebb periods it is seen that the computed salinities show well-mixed distribution in the gulf channel. For suspended sediment transport numerical experiments are performed by taking three settling velocities, namely 3.4 x 10^{-3}ms^{-1} (very fine sand), 8.8 x 10^{-4} ms^{-1} (coarse silt) and 5.5 x 10^{-5} ms^{-1} (fine silt).

2 Governing Equations

The origin 'O' of a system of rectangular Cartesian coordinate has been taken at the equilibrium level of the free surface in the gulf (Figure 2). Ox points seaward and Oz is measured vertically upward from z = 0. The landward end has been taken at x = 0 and the seaward end is denoted by x = L. The elevations of the free surface above its mean level is denoted by $z = \zeta(x,t)$ and the bottom topography by z = -h(x). The breadth of the gulf at position x is denoted by b(x). The Reynold's-averaged components of the fluid velocity and fluid density are denoted by (u,w) and ρ, respectively.

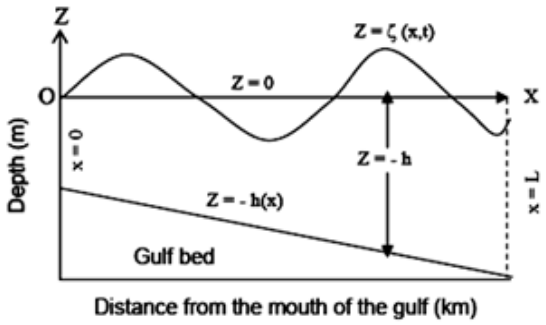

Figure 2: Model Geometry and Coordinate System

By invoking Boussinesq and hydrostatic approximations, the breadth-averaged momentum equation can be written as (Johns and Oguz, [2])

$$\frac{\partial}{\partial t}(bu)+\frac{\partial}{\partial x}(bu^2)+\frac{\partial}{\partial z}(buw) = \text{-gb}\frac{\partial \zeta}{\partial \text{x}}-\frac{b}{\rho_0}\int_z^{\zeta}\frac{\partial}{\partial x}(g\rho)dz+\frac{\partial}{\partial z}\left(K_M\frac{\partial(bu)}{\partial z}\right)+\frac{\partial}{\partial x}\left(bN\frac{\partial u}{\partial x}\right) \quad (1)$$

The first term on the right hand side of equation (1) gives the barotropic contribution to the pressure gradient resulting from the slope of the free surface in the channel. The second term, in which ρ_0 is the density of the fresh water, gives the baroclinic contribution to the pressure gradient. The third term represents the vertical transfer of momentum by turbulent motions and is expressed in terms of conventional gradient law involving a vertical coefficient of viscosity, K_M. The last term represents the effect of horizontal momentum exchange by turbulent scale motions where N is the horizontal eddy transfer coefficient.

The equation of continuity is expressed either as

$$\frac{\partial u}{\partial x} + \frac{\partial w}{\partial z} = 0 \tag{2}$$

or

$$\frac{\partial \zeta}{\partial t} + \frac{\partial}{\partial x}(H\overline{u}) = 0 \tag{3}$$

where H ($= \zeta + h$) is the total depth and $\overline{u}$ is the depth-averaged velocity given by

$$\overline{u} = \frac{1}{H}\int_{-h}^{\zeta} u dz \tag{4}$$

The density ρ is related to the sediment concentration, C, given by (Johns et al., [4])

$$\rho = \rho_0 \left(1 + \Gamma C\right) \tag{5}$$

where

$$\Gamma = \left(\frac{1}{\rho_0} - \frac{1}{\rho_s}\right) \tag{6}$$

and ρ_s is the density of a single grain size of sediment.

The salinity is determined from a transport equation having the form

$$\frac{\partial}{\partial t}(bS) + \frac{\partial}{\partial x}(buS) + \frac{\partial}{\partial z}(bwS) = \frac{\partial}{\partial z}\left[K_s \frac{\partial}{\partial z}(bS)\right] + \frac{\partial}{\partial x}\left[bN\frac{\partial S}{\partial x}\right] \tag{7}$$

On the right-hand-side of equation (7), the first term represents the vertical transfer of salinity by turbulent processes in terms of gradient transfer law with an eddy coefficient, K_s. The second term simulates the effect of horizontal salinity flux by turbulent scale motions.

The advection-diffusion equation for suspended sediment concentration is given by

$$\frac{\partial}{\partial t}(bC) + \frac{\partial}{\partial x}(buC) + \frac{\partial}{\partial z}(bwC) = \frac{\partial}{\partial z}\left(K_C \frac{\partial}{\partial z}(bC)\right) + \frac{\partial}{\partial x}\left(bN\frac{\partial C}{\partial x}\right) + \gamma w_s(C_e - C) \tag{8}$$

where γ is the profile factor given by $\gamma = C_{-h}/C$, $w_s$is the sediment settling velocity, C_e is the equilibrium concentration and K_C is the vertical eddy diffusion coefficient for sediment concentration.

The turbulence energy density, E, is determined from the equation (Johns and Oguz, [2])

$$\begin{aligned}\frac{\partial}{\partial t}(bE) + \frac{\partial}{\partial x}(buE) + \frac{\partial}{\partial z}(bwE) = {} & bK_M\left(\frac{\partial u}{\partial z}\right)^2 + bN\left(\frac{\partial u}{\partial z}\right)^2 + \frac{g}{\rho_0} bK_\rho \frac{\partial \rho}{\partial z} \\ & + \frac{\partial}{\partial z}\left[K_E \frac{\partial}{\partial z}(bE)\right] + \frac{\partial}{\partial x}\left[bN\frac{\partial E}{\partial x}\right] - b\varepsilon\end{aligned} \tag{9}$$

where K_E, K_ρ are the exchange coefficients for turbulence energy density and density, respectively. The first term on the right hand side of equation (9) represents the production of turbulence energy due to vertical shear in Reynold's averaged flow. The second term represents the production of turbulence energy associated with the action of normal eddy stress. The third term gives the positive or negative contribution of E depending upon the vertical density stratification. The fourth term represents the vertical diffusion of turbulence energy with an eddy coefficient, K_E. The fifth term represents the horizontal distribution of turbulence itself. The last term simulates the dissipation of turbulence energy.

The various eddy coefficients appearing in the formulation are expressed in terms of the turbulence energy density. In the present work, we choose

$$K_M = K_S = K_C = K_E = K \tag{10}$$

where

$$K = c^{\frac{1}{4}}\ \ell\ E^{\frac{1}{2}} \tag{11}$$

Here, $c = 0.08$ is an empirical coefficient (Launder and Spaulding, [8]) and ℓ is the vertical mixing length scale given by

$$\ell = \ell_0\ \exp\left[\ -\ \frac{1}{4}\beta(z+h)\right] \tag{12}$$

Following Johns [3], ℓ_0 is determined by

$$\ell_0 = \frac{K\frac{E^{\frac{1}{2}}}{\ell_0}}{\frac{d}{dz}(\frac{E^{\frac{1}{2}}}{\ell_0})}, \quad \ell_0 = \kappa\ z_0 \text{ at z } =\ \text{-h} \tag{13}$$

where, κ is the Von Karman's constant, and z_0 is the roughness length at the floor of the gulf channel. In equation (12), β has an inverse length scale, which is included to overcome the possibility of over mixing in the vertical direction.

The dissipation term, ε, in equation (7), is parameterized by writing

$$\varepsilon = \frac{c^{3/4}E^{3/2}}{\ell_D} \tag{14}$$

where the dissipation length scale, ℓ_D, is given by

$$\ell_D = \ell_0 \exp\left[\frac{3}{4}\beta(\text{z} + \text{h})\right] \tag{15}$$

The horizontal eddy transfer coefficient, N, is parameterized based on dimensional consideration as

$$N = \alpha\Delta x E^{\frac{1}{2}} \tag{16}$$

where the grid increment, Δx, is taken as the horizontal mixing length scale and α is a disposable parameter.

3 Boundary Conditions

The above equations are accompanied by appropriate boundary conditions. At the floor of the gulf a no-slip condition has been applied. Further, no diffusive flux of salinity across the floor of the gulf is considered. At the free surface, the applied wind stress and diffusive salinity flux are taken as zero. Also, the vertical exchange of turbulence energy across the floor and the surface of the gulf channel is taken as zero.

Thus, the fluid motion in the channel is driven solely by the boundary forcing to be applied at the extremities of the channel. In the present application tidal condition has been specified based on observations at the seaward end ($x = L$) as

$$\zeta = \sum_{i=1}^{n} a_i \cos(\omega t + \phi_i) \tag{17}$$

where a_i and ϕ_i are the amplitude and phase of the i-th tidal constituent.

At the landward end a radiation boundary condition is applied which takes care of the outward transmission of the disturbances in the form of a simple progressive wave. The freshwater discharge through the gulf may be achieved by prescribing

$$\overline{u} + \left(\frac{g}{h}\right)^{1/2} \zeta = 2u_0 \tag{18}$$

where u_0 is a constant velocity that determines the strength of the fresh water flow. To allow the information about the salinity structure within the gulf, it is necessary that the boundary conditions to accompany equation (7) be correctly formulated. Essentially, the conditions to be applied at $x = 0$ and $x = L$ must be such that the salinity of inflowing water is prescribed and the outflowing water is determined by use of equation (7).

Therefore, during inflow, the conditions are given by

$$S = S_0 \text{ at } x = 0, \text{ when } u > 0 \tag{19}$$

and during outflow, the conditions are given by

$$S = S_L \text{ at } x = L, \text{ when } u < 0. \tag{20}$$

Here, $S_0$and S_L are observed salinities at the landward end and seaward end, respectively.

Boundary conditions on C are of special importance. Here, we prescribe that there is no flux of sediment concentration across the free surface. Bearing in mind that the total upward flux consists of an advective, a settling and a diffusive contribution, this leads to the requirement that

$$(w - w_s)C = K\frac{\partial C}{\partial z} \text{ at z} = \zeta \tag{21}$$

The boundary condition on C at the bed utilizes the parameterization of upward diffusive flux in terms of an empirically based pick-up function suggested by Van Rijn [9]. In our applications, this leads to

$$\left(-K\frac{\partial C}{\partial z}\right) = C_0(\delta\ g\ D_{50})^{\frac{1}{2}}\theta^{\frac{3}{2}} \text{ at z} = \text{-h} \tag{22}$$

$$\theta = \left\{ \begin{array}{l} 0 \; for \; u_* < u_{*c} \\ \left(u_*/u_{*c}\right)^2 - 1 \; for \; u_* > u_{*c} \end{array} \right\} \tag{23}$$

where u_* is the bottom friction velocity and u_{*c} is the critical bottom friction velocity for the onset of sediment pick-up as determined by Van Rijn [9]. C_0 is a reference concentration density given by

$$C_0 = 0.00033 \; \rho_s \; D_*^{0.3} \tag{24}$$

$$D_* = D_{50}(\delta \; g/\nu^2)^{\frac{1}{2}}, \tag{25}$$

in which D_{50} is the grain diameter, $\nu$is the kinematic viscosity and

$$\delta = (\rho_s - \rho)/\rho \tag{26}$$

4 Coordinate Transformation

A non-dimensional vertical coordinate, σ, is introduced to facilitate the representation of the boundary conditions accurately at z = -h(x) and $z = \zeta$(x,t). We take

$$\sigma = \frac{z+h}{H} \tag{27}$$

so that σ increases monotonically from $\sigma = 0$ at the floor of the gulf to $\sigma = 1$ at the free surface. A new dependent variable, ω, is defined by

$$\omega = \frac{D\sigma}{Dt} = \frac{\partial \sigma}{\partial t} + u\frac{\partial \sigma}{\partial x} + w\frac{\partial \sigma}{\partial z} \tag{28}$$

which is zero at both the gulf floor and the free surface. The new prognostic variables are given by

$$\left(\tilde{u}, \tilde{S}, \tilde{E}, \tilde{C}\right) = bH\left(u, S, E, C\right) \tag{29}$$

$$\frac{\partial \tilde{u}}{\partial t} + \frac{\partial}{\partial x}\left(u\tilde{u}\right) + \frac{\partial}{\partial \sigma}\left(w\tilde{u}\right) = -gbH\frac{\partial \zeta}{\partial x} - g\Gamma bH^2\int_0^1 \frac{\partial C}{\partial x}d\sigma + g\Gamma bH\left\{\left(\left(1-\sigma\right)C - \int_0^1 C d\sigma\right)\frac{\partial h}{\partial x}\right\}$$

$$+\left(C_{\sigma=1} - \sigma C - \int_0^1 C d\sigma\right)\frac{\partial \zeta}{\partial x} + \frac{1}{H^2}\frac{\partial}{\partial \sigma}\left(K\frac{\partial \tilde{u}}{\partial \sigma}\right) + \frac{\partial}{\partial x}\left(bHN\frac{\partial u}{\partial x}\right) \tag{30}$$

$$\frac{\partial}{\partial x}\left(u - \bar{u}\right) + \frac{\partial}{\partial \sigma}\left(bH\omega\right) = 0 \tag{31}$$

$$\frac{\partial \tilde{S}}{\partial t} + \frac{\partial}{\partial x}\left(u\tilde{S}\right) + \frac{\partial}{\partial \sigma}\left(\omega\tilde{S}\right) = \frac{1}{H^2}\frac{\partial}{\partial \sigma}\left(K\frac{\partial \tilde{S}}{\partial \sigma}\right) + \frac{\partial}{\partial x}\left(bhN\frac{\partial S}{\partial x}\right) \tag{32}$$

$$\frac{\partial \tilde{C}}{\partial t} + \frac{\partial}{\partial x}\left(u\tilde{C}\right) + \frac{\partial}{\partial \sigma}\left[\left(w - w_s\right)\tilde{C}\right] = \frac{1}{H^2}\frac{\partial}{\partial \sigma}\left(K\frac{\partial \tilde{C}}{\partial \sigma}\right) + \frac{\partial}{\partial x}\left(bhN\frac{\partial C}{\partial x}\right) + \frac{\gamma w_s}{H}\left(bHC_e - \tilde{C}\right) \tag{33}$$

$$\frac{\partial \tilde{E}}{\partial t}+\frac{\partial}{\partial x}\left(u\tilde{E}\right)+\frac{\partial}{\partial \sigma}\left(\omega\tilde{E}\right)=\frac{bK}{H^3}\left(\frac{\partial \tilde{u}}{\partial \sigma}\right)^2+gbK\Gamma\frac{\partial C}{\partial \sigma}+bHN\left(\frac{\partial u}{\partial x}\right)^2+\frac{1}{H^2}\frac{\partial}{\partial \sigma}\left(K\frac{\partial \tilde{E}}{\partial \sigma}\right)+\frac{\partial}{\partial x}\left(bHN\frac{\partial E}{\partial x}\right)-bH\varepsilon \tag{34}$$

The boundary conditions to accompany the set of transformed equations are

$$\left.\begin{aligned}\omega_{\sigma=0,1}&=0\\ u_{\sigma=0}&=0\\ \frac{\partial u}{\partial \sigma}_{\sigma=1}&=0\\ K\frac{\partial E}{\partial \sigma}_{\sigma=0,1}&=0\\ K\frac{\partial S}{\partial \sigma}_{\sigma=0,1}&=0\end{aligned}\right\} \tag{35}$$

The boundary condition (17) has an unchanged form, but the depth-averaged velocity, $\overline{u}$ is given by

$$\overline{u}=\int_0^1 u\ \mathrm{d}\sigma \tag{36}$$

The basic length scale given by equation (13) is transformed to

$$\ell_0=\kappa z_0(\frac{E}{E_b})+\kappa E^{\frac{1}{2}}H\int_0^{\sigma}E^{-1/2}d\sigma \tag{37}$$

The boundary conditions for the sediment concentration transform to

$$(w-w_s)\ C=\frac{K}{H}\frac{\partial C}{\partial \sigma}\quad \text{at}\quad \sigma=1 \tag{38}$$

$$\left(-\frac{K}{H}\frac{\partial C}{\partial \sigma}\right)=C_0\left(\delta\ g\ D_{50}\right)^{1/2}\theta^{1/2}\ \text{ at }\ \sigma=0 \tag{39}$$

5 Numerical Experimentation

The predictive equations (30) to (34) are solved numerically by considering a discrete set of grid points defined by

$$\begin{aligned}&x=x_i=(i-1)\,\Delta x\quad i=1,2,\ldots,m\\ &\sigma=\sigma_k=(k-1)\,\Delta\sigma\quad k=1,2,\ldots,n\\ &t=t_p=p\Delta t\quad p=0,1,2,\ldots\end{aligned} \tag{40}$$

where $\Delta x=L/(m-1)$ and $\Delta\sigma=1/(n-1)$ are the grid increments in the horizontal and vertical directions, respectively, and L is the length of the analysis area.

Computations are carried out on a staggered grid in the horizontal direction, and an un-staggered grid in the vertical. In the horizontal direction, if i is odd, the dependent variables ζ, S and C are evaluated, and when i is even, u, E, ℓ and K are computed. m is chosen to be odd so that the end points of the computational domain correspond to ζ-points.

For the present study the analysis area of the gulf of Kachchh extends from 68.93^0 E to 70.04^0 E and 22.23^0 N to 22.87^0 N (Figure 1). Due to the presence of creeks at the landward end namely, Nakti creek, Khori creek and Kandla creek it is difficult to average the region in terms of breadths. So we considered the landward-end of the analysis region at about 70.04^0 E. We have chosen the length of the channel to be 123 km and the breadth decreases from 64.5 km at the mouth to about 36 km at the upstream end. The mean centre-line depth has been taken as the representative bathymetry for this study (Figures 3a – 7b). The selection of 83 computational points in the x-direction results in a horizontal grid distance of 1.5 km. The prescription of 49 computational levels in the vertical provides a vertical grid distance of 0.31 m in the shallow region and 1.04 m in the region of maximum depth. Since the tidal forcing is an important feature of the present study, a realistic boundary condition based on observations is used. Accordingly, a boundary condition for M_2 tide has been prescribed as (Unnikrishanan et al., [10])

$$\zeta_{x=L} = 1.24 \cos\left(\frac{2\pi t}{T} - 205^o\right) \tag{41}$$

The salinity boundary conditions are prescribed on the basis of observations as $S_0 = 39.3$ psu and $S_L = 35.8$ psu (Sen Gupta and Deshmukhe, [11]). For suspended sediment transport numerical experiments are carried out by taking three settling velocities, namely, 3.4 x 10^{-3} ms^{-1} (very fine sand), 8.8 x 10^{-4} ms^{-1} (coarse silt) and 5.5 x 10^{-5} ms^{-1} (fine silt). The corresponding diameters of the sediment grains are 0.125 mm, 0.062 mm and 0.016 mm, respectively. Having fixed the horizontal grid distance, the attainment of computational stability in the solution process is conditional only upon the time step. A time step of 30 seconds is found to be consistent with the computational stability. Thus, starting from an initial state of rest, the governing equations are integrated forward in time till a steady state is reached.

6 Results and Discussion

The final predictive equations (30) to (34) are solved subject to appropriate initial and boundary conditions. The steady state is reached in 8^{th} tidal cycle and the results of the 9^{th} tidal cycle are analysed. The results shown in Figures 3 to 7 are presented in a vertical transect in the middle of the channel.

Figures 3a and 3b show the tidal currents along the channel during flood and ebb periods, respectively. The results clearly indicate that the currents are either flood-directed or ebb-directed for the respective tidal periods. The maximum current velocity during flood is 2 $ms^{-1}$and that during ebb is 1.96 ms^{-1}. In these figures the contours indicates the magnitude of the velocities in the gulf regions. Also, the current was computed in a vertical transect at three levels (surface, mid-depth and bottom) and at three locations (seaward, mid-way and landward) of the analysis area. The seaward, mid-way and landward stations correspond to approximately 68.93^0E, 69.48^0 E and 70.04^0 E. The seaward flood currents

at the surface, mid-depth and bottom are 2 ms^{-1}, 1.1 ms^{-1} and 0.5 ms^{-1}, respectively. At the middle station, the corresponding values are 1.3 ms^{-1}, 0.9 ms^{-1} and 0.4 ms^{-1}while at the landward station, the values are 1 ms^{-1}, 0.6 ms^{-1} and 0.3 ms^{-1}.

Similarly, the respective seaward ebb currents at the three levels are 1.96 ms^{-1}, 1 ms^{-1} and 0.45 ms^{-1}; in the mid-way these values are 1.2 ms^{-1}, 0.8 ms^{-1} and 0.3 ms^{-1} and at the landward station the values are 1 ms^{-1}, 0.5 ms^{-1} and 0.25 ms^{-1}.

The computed salinity profiles are shown in Figures 4a and 4b during flood and ebb periods, respectively. During flood the surface salinity increases from the mouth (35.98 psu) to upstream end (39.2 psu). The computed surface salinity during ebb varies from 34 psu at the seaward end to 35 psu at the landward-end. In the middle region of the gulf the salinity varies from 37 psu to 39 psu. During both the periods it is seen that the computed salinities show well-mixed distribution in the gulf channel.

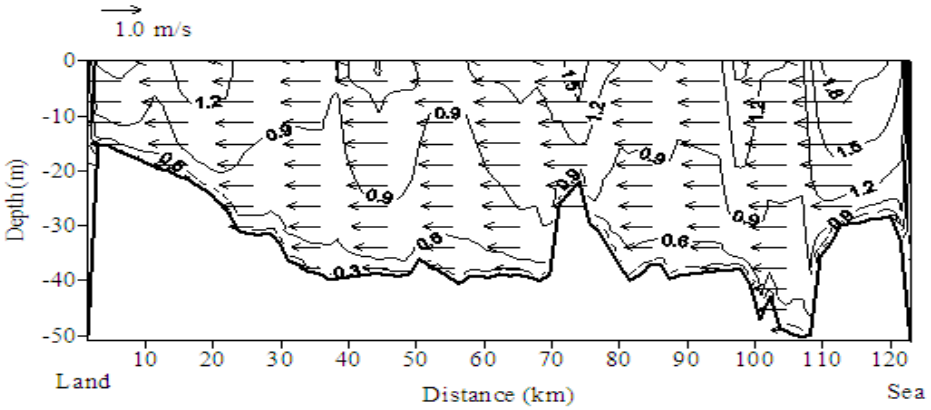

Figure 3(a): Tidal Currents Along the Gulf of Kachchh during Flood. Contours Indicate Current Magnitude (m/s)

Some observations of salinity values are available at surface and bottom of the three stations, namely Okha, Karumbhar and Mundra which are about 117 km, 52 km and 36 km from the landward end, respectively. Therefore, salinity was computed at the surface and the bottom of the three stations in the channel. At Okha, the computed salinity values at the surface and the bottom are 36.09 psu and 36.13 psu, respectively. The corresponding values at Karumbhar are 38.16 psu and 38.19 psu while at Mundra, the values are 38.52 psu and 38.54 psu. However, during the ebb period the computed surface salinities at the corresponding stations are 35.20 psu, 38.45 psu and 38.73 psu and at the bottom these values are 35.22 psu, 38.48 psu and 38.77 psu, respectively.

The computed results for the flood period are validated at these three stations with the available observations (Table 1). It is found that the salinities are in agreement with the observed/estimated values (Sen Gupta and Deshmukhe, [11]).

The computed results show that the salinity increased from the mouth to the upstream end and the vertical profiles indicate well-mixed distribution in the gulf region. Unnikrishnan et al. [10] have reported that the salinity near the mouth is about 36 psu while inside the gulf it has a higher value of about 40 psu. Because of the high annul rate of

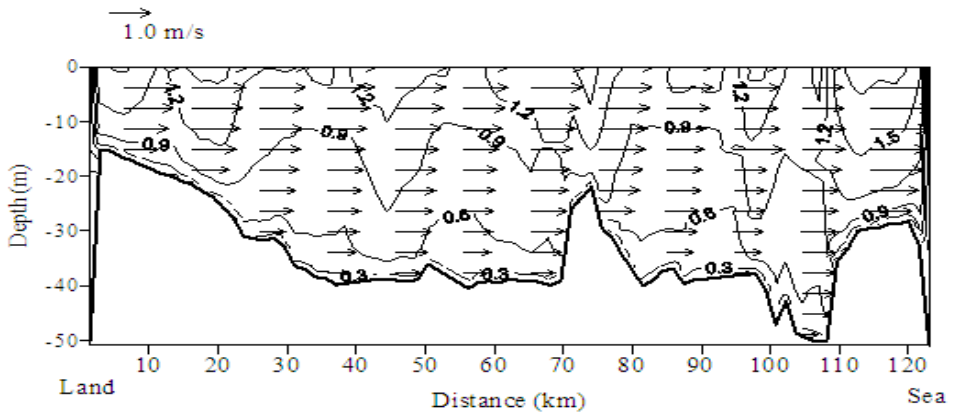

Figure 3(b): Tidal Currents Along the Gulf of Kachchh during Ebb. Contours Indicate Current Magnitude (m/s)

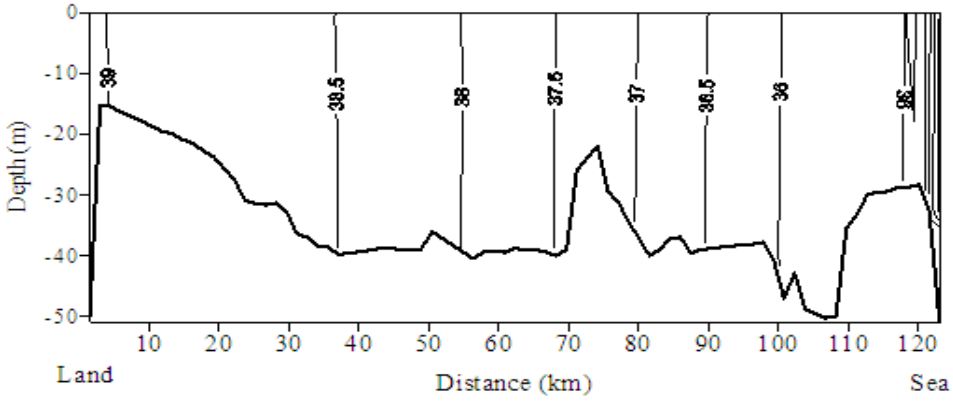

Figure 4(a): Salinity Profiles (psu) along the Gulf of Kachchhj During Floods

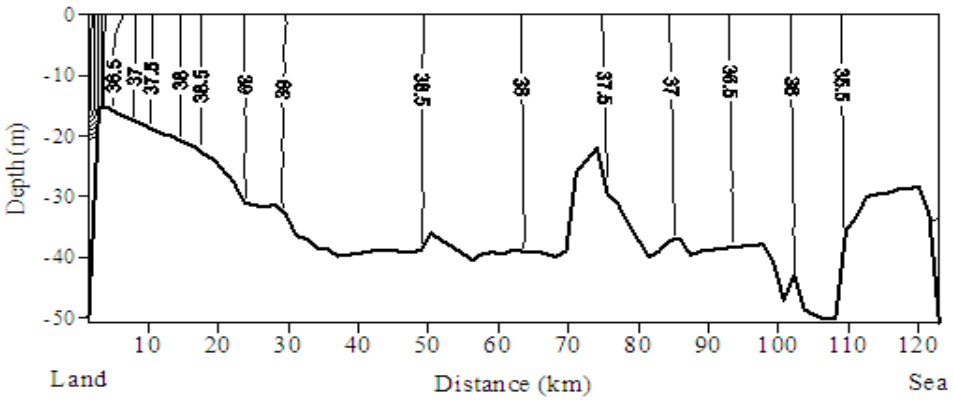

Figure 4(b): Salinity Profiles (psu) along the Gulf of Kachchhj During Ebb

Table 1: Observed and computed salinities during flood at the surface and the bottom of three stations in the gulf of Kachchh.

Stations	Observed salinity range	Mean salinity	Computed salinity
Okha	Surface 35.27 - 36.39 Bottom 35.72 - 36.45	35.83 36.08	36.09 36.13
Karumbhar	Surface 36.26 - 37.86 Bottom 36.68 - 36.91	37.06 36.79	38.16 38.19
Mundra	Surface 37.15 - 37.48 Bottom 37.22 - 37.69	37.31 37.45	38.52 38.54

evaporation minus precipitation and low runoff, salinities are higher in the gulf than at the mouth. Available salinity data suggest that the gulf is vertically well-mixed.

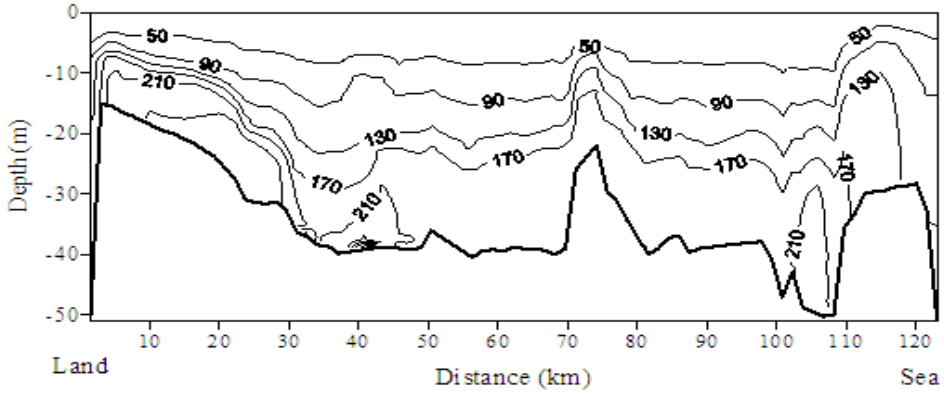

Figure 5(a): Suspended Sediment Concentratiopns for Very Fine Sand (mg/l) along the Gulf of Kachchh During Flood

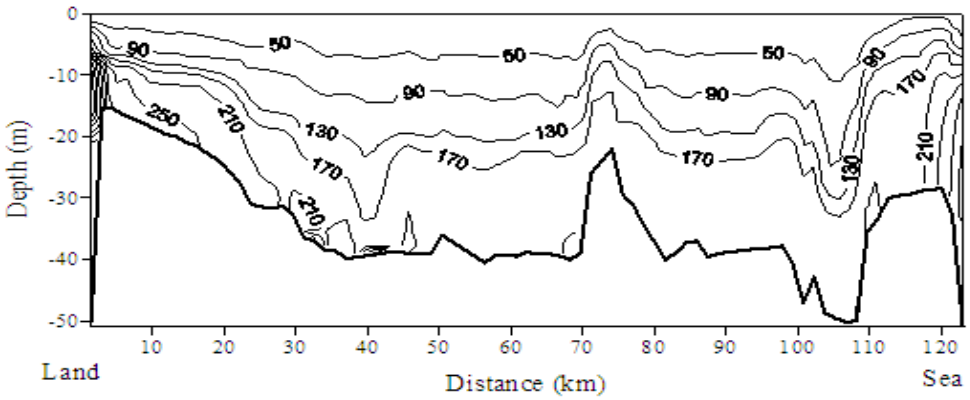

Figure 5(b): Suspended Sediment Concentratiopns for Very Fine Sand (mg/l) along the Gulf of Kachchh During Ebb

The computed suspended sediment concentrations for very fine sand (w_s= 3.4 x 10^{-3} ms^{-1}) are shown in Figures 5a and 5b for flood and ebb periods, respectively. The sediment concentrations vary from 12 mg/l to 247 mg/l during flood and from 12 mg/l to 250 mg/l during the ebb period. As expected the computed concentrations increase from the surface towards the bottom. The suspended sediment contours follow the bathymetry of the analysis area. Figures 6a and 6b depict the computed suspended sediment transport for the coarse silt (w_s= 8.8 x 10^{-4} ms^{-1}) during flood and the ebb periods, respectively. The sediment concentrations during flood vary from 10 mg/l to 214 mg/l and during ebb it is found to

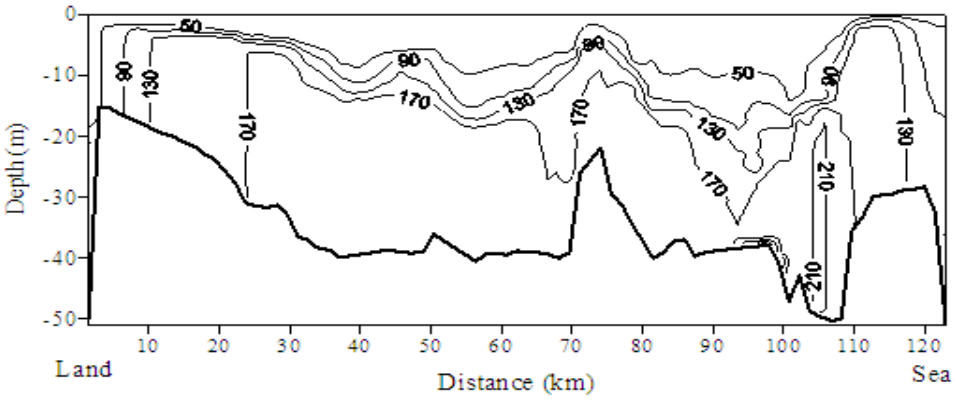

Figure 6(a): Suspended Sediment Concentratiopns for Fine Sand (mg/l) along the Gulf of Kachchh During Flood

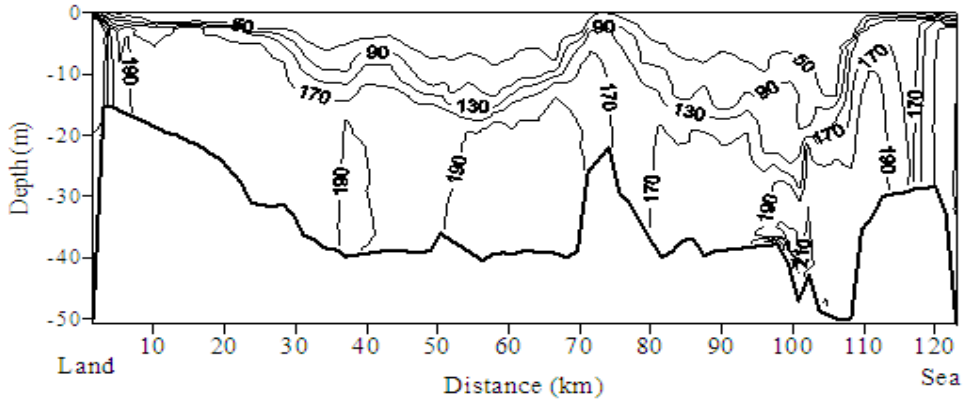

Figure 6(b): Suspended Sediment Concentratiopns for Very Sand (mg/l) along the Gulf of Kachchh During Ebb

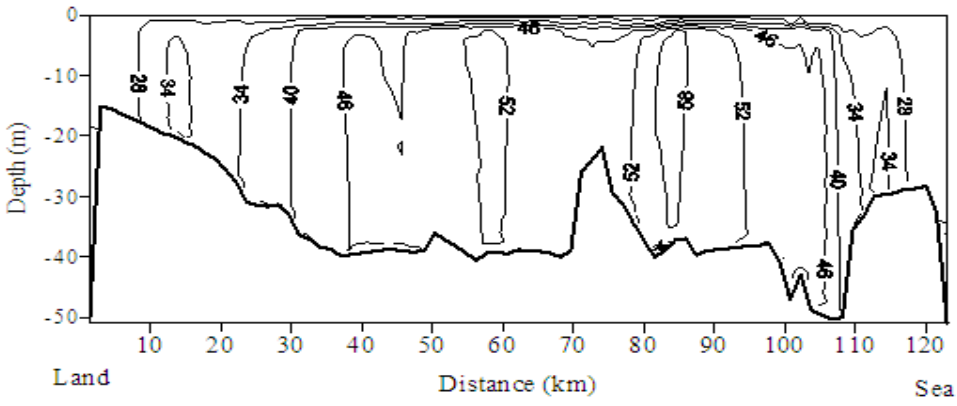

Figure 7(a): Suspended Sediment Concentratiopns for Coarse Silt (mg/l) along the Gulf of Kachchh During Flood

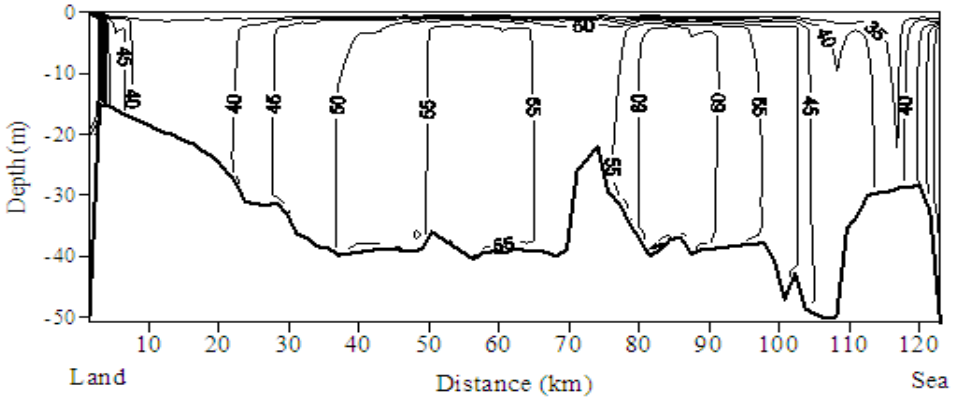

Figure 7(b): Suspended Sediment Concentratiopns for Coarse Silt (mg/l) along the Gulf of Kachchh During Ebb

vary from 10 mg/l to 110 mg/l. Similarly, the computed sediment concentrations for fine silt (w_s = 5.5 x 10^{-5} ms^{-1}) for flood and ebb periods as shown in Figures 7a and 7b, respectively. During the flood period, the concentrations vary from 10 mg/l to 58 mg/l and it varies from 10 mg/l to 65 mg/l for the ebb period. The results clearly indicate that the sediment concentrations decrease as we move from higher to lower values of the settling velocities.

7 Conclusions

A multilevel breadth-averaged numerical model has been developed to study the tidal circulation, salinity intrusion and suspended sediment transport in the gulf of Kachchh along the west coast of India. Details of the formulation and numerical procedure are described in this study. For the parameterization of turbulent diffusivity and vertical eddy viscosity, a turbulence closer scheme has been used in the model. This involves the parameterization of Reynold's stress in terms of turbulence energy density and velocity shear. Several experiments are carried out for the tidal circulation and salinity distribution in the gulf. The simulated salinity profiles show realistic fully mixed distribution in the analysis region. The salinity results are validated for the flood period at the surface and the bottom of three stations, namely, Okha, Karumbar and Mundra. It is found that the computed salinities are in agreement with the available observations. Also, experiments are conducted for suspended sediment concentrations in the gulf by taking three settling velocities, w_s= 3.4 x 10^{-3} ms^{-1}, w_s= 8.8 x 10^{-4} $ms^{-1}$and w_s = 5.5 x 10^{-5} m/s. As expected the sediment concentrations are higher for higher values of the settling velocities.

References

[1] Central Electricity Authority, *Investigations and Studies for Tidal Power Development in the Gulf of Kutch*, Interim Rep. Ministry of Irrigation and Power, Govt. of India, New Delhi, 1985.

[2] B. Johns & T. Oguz, *The Modeling of Flow of Water Through the Bosphorous*, Dyn. Atmos. Oceans, 14(1990), 229–258.

[3] B. Johns, *The Modeling of Tidal Flow in a Channel Using a Turbulence Energy Closer Scheme*, J. Phys. Oceanogr., 8(1978), 1042–1049.

[4] B. Johns, R.L. Soulsby & T.J. Chesher, *The Modeling of Sandwave Evolution Resulting from Suspended and Bedload Transport of Sediment*, J. Hydr. Research, 28(1990), 355–374.

[5] Wen-Cheng, Liu, Ming-His, Hsu, Chi-Ray Wu, Chi-Fang Wang & Albert Y. Kuo, *Modeling Salt Water Intrusion in Tanshui River Estuarine System- Case Study Contrasting Now and Then*, J. of Hydr. Engg., ASCE, 130(2004), 849–859.

[6] D. Prandle, *Saline Intrusion in Partially Mixed Estuaries*, *Estuarine,* Coastal and Shelf Science, 54(2004), 385–397.

[7] X.J. Chen, *Modeling Hydrodynamics and Salt Transport in the Alafia River Estuary, Florida During May 1999-December 2001*, Estuarine, Coastal and Shelf Science, 1(2004), 477–490.

[8] B.E. Launder & D.B. Spaulding, *Lectures in Mathematical Model of Turbulence,* Academic press, New York, 1972.

[9] L.C. Van Rijn, *Application of Sediment Pick-up Function*, J. Hydr. Engg., ASCE, 10(1966), 507–514.

[10] A.S. Unnikrishnan, A. D. Gouveia, & P. Vethamony, *Tidal Regime in Gulf of Kutch, West Coast of India, by 2D Model*, J. Waterway, Port, Coastal, and Ocean Engg., 125(1999), 276–284.

[11] R. Sen Gupta & G. Deshmukhe, *Coastal and Maritime Environment of Gujarat*, Gujarat Ecological Society, Vadodara, India, 2000.